ELSEVIER

International Journal of Mass Spectrometry 223–224 (2003) 539–546

International Journal of Mass Spectrometry

www.elsevier.com/locate/ijms

The reaction of SiH^+ and SH^+ with small molecules

J. Glosík[a,*], P. Zakouřil[a], A. Luca[a,b]

[a] *Department of Electronics and Vacuum Physics, Mathematics and Physics Faculty, Charles University, V Holešovičkách 2, Prague 8, Czech Republic*

[b] *Institut für Physik, Technische Universität, 09107 Chemnitz, Germany*

Received 18 February 2002; accepted 8 June 2002

We dedicate this paper to memory of our dear late friend Werner Lindinger.

Abstract

The kinetics of the reactions of the ion SH^+ with CH_4 and C_2H_2 and SiH^+ with C_2H_2 and NH_3 has been investigated using selected ion flow drift tube technique (SIFDT). The reaction rate coefficients and the products branching ratio have been determined as a functions of the reactant ion/reactant neutral average centre-of-mass kinetic energy (KE_{CM} = 0.05–2 eV). The studied reactions are fast at thermal and near thermal energies and have negative energy dependencies of the reaction rate coefficients. (Int J Mass Spectrom 223–224 (2003) 539–546)

Keywords: Ion–molecule reaction; Reaction rate coefficient; SH^+; SiH^+

1. Introduction

During the past decades, there has been considerable interest in the chemistry of silicon and sulfur bearing compounds. Many silicon-bearing ions, their structure, thermochemistry, and their reactions with neutral molecules have been subject of a number of theoretical as well as experimental studies (e.g. [1–4] and references therein). The reactivity and structure of some sulfur-bearing ions have also been the subject of a few recent studies (e.g. [5–7]). Studies of ion–molecule reactions of silicon- and sulfur-bearing ions, SiH^+ and SH^+ in particular, are mostly motivated by the importance of these reactions in interstellar clouds [8–12]. Recently, we have made selected ion flow drift tube technique (SIFDT) studies of reactions of several Si and S bearing ions with molecules looking for energy dependencies of rate coefficients, products and branching ratios of these reactions (e.g. [2,13–15]). See also the review by Bohme [16], the compilation of Anicich [17] and references therein.

Because of the low ionization potential of Si and S, the reactions of silicon and sulfur bearing ions are often proceeding via formation of the long-lived collision complexes. For example, in reactions of Si^+ with small molecules charge transfer or dissociative charge transfer are essentially excluded because of the low ionization potential of Si (only 8.15 eV). The reactions are usually proceeding by incorporating of Si^+ into the molecular product ion. This requires a rearrangement of existing bonds within the reactant molecule and formation of new bonds. The probability of such processes increases when a long-lived intermediate complex is formed. The mechanism of

* Corresponding author. E-mail: juraj.glosik@mff.cuni.cz

1387-3806/02/$ – see front matter
PII S1387-3806(02)00875-8

such reactions is reflected in its kinetics. The increasing internal energy accumulated in a complex can lead to a decrease of the lifetime of this complex towards dissociation back to the reactants and an eventual decrease of the reaction rate coefficient. This will be reflected in a negative energy dependence of a reaction rate coefficient. This description is oversimplified, for details we refer the reader to articles of Dunbar [18], Troe [19], Klots [20], and Forst [21]. In the drift tube, the energy brought to the reaction is determined by the temperature of the buffer gas and by the intensity of the axial electric field.

For several recent years our research has been directed towards description and understanding of the ion–molecule reactions of this type (e.g. [2,13–15,22,23]). The reported reactions of the ion SiH^+ and SH^+ are also from this category.

The reactions proceeding via formation of an intermediate reaction complex can be described by the following reaction scheme:

$$A^+ + B \underset{k_{-1}}{\overset{k_1}{\leftrightarrow}} (AB^+)^* \overset{k_2}{\rightarrow} C^+ + D \quad (1)$$

where $(AB^+)^*$ is an intermediate reaction complex and k_1, k_{-1} and k_2 are reaction rate coefficients corresponding to indicated processes. The decay towards products characterized by k_2 can have for particular reactants several channels. By applying simple reaction kinetics and applying the steady-state approximation to $(AB^+)^*$, the following expression is obtained for the overall rate coefficient k of the reaction (1):

$$k = k_1 \frac{k_2}{k_{-1} + k_2} = k_1 \frac{1}{1 + (k_{-1}/k_2)} \quad (2)$$

From this relation it is evident that if k_1 is a constant, the ratio (k_{-1}/k_2) and its dependence on KE_{CM} governs the energy dependence of the overall reaction rate coefficient k (as long as the assumption concerning the complex formation is valid). For many ion–molecule reactions k_1 is equal to the capture rate coefficient (k_C) or a fixed fraction. The assumption that intermediate complex is formed at the capture rate ($k_1 = k_C$) is very common in analysis of the kinetics of ion–molecule interactions (e.g., in discussions of vibrational quenching by Ferguson [24]). We will not consider here small increase of capture rate coefficient when KE_{CM} is increasing over 1 eV (see discussion of this phenomenon in our previous work [2]).

In analogy with the ideas used for three-body association reactions, where long-lived intermediate complexes are formed and play a substantial role, we assume here that k_{-1}/k_2 is proportional to centre-of-mass kinetic energy $(KE_{CM})^m$, where m is a constant. With this assumption, we can use substitution $k_{-1}/k_2 = (KE_{CM}/KE_{CM1})^m$, where $(1/KE_{CM1})^m$ is constant of proportionality (the meaning of KE_{CM1} will be discussed in the following sections, see also discussion in appendix of [25,26], where concept of effective temperature and its relation to KE_{CM} is also discussed). The overall reaction rate coefficient can then be written as:

$$k = k_1 \frac{1}{1 + (KE_{CM}/KE_{CM1})^m} \quad (3)$$

The parameters (constants) m, KE_{CM1} and k_1 can be determined from the fit of the plot of measured rate coefficient k vs. KE_{CM}. On the other hand, if the measured dependence of k on KE_{CM} can be approximated by a function (3), it can be a good reason to assume that such a reaction is proceeding via formation of long-lived intermediate complex and can be characterized by the reaction scheme (1). As can be seen from Eq. (3), the parameter KE_{CM1} is equal to KE_{CM} at which character of the energy dependence is changed, from $k \sim k_1$ (for $1 \gg (KE_{CM}/KE_{CM1})^m$) to $k \sim k_1(KE_{CM1}/KE_{CM})^m k_1$ (for $1 \ll (KE_{CM}/KE_{CM1})^m$). In another words, for $KE_{CM} < KE_{CM1}$ the formation of a collisional complex is a rate determining step, for $KE_{CM} > KE_{CM1}$ the value of KE_{CM} starts to influence the rate of the overall reaction.

The used assumption $k_{-1}/k_2 \sim (KE_{CM})^m$ can be supported also on the basis of statistical arguments (e.g., discussion in [27]). In order to visualize the "power law dependence" given by Eq. (3), it can be rewritten to the form:

$$\frac{k_1}{k} - 1 = \frac{k_{-1}}{k_2} = \left(\frac{KE_{CM}}{KE_{CM1}}\right)^m \quad (4)$$

Here k is the measured quantity, and we assume that k_1 can be obtained as a limiting value of k at low

KE_{CM}. The linearity of the log-log plot of $((k_1/k) - 1)$ vs. KE_{CM} then can serve as justification of our assumption that the reaction proceeds via formation of an intermediate complex.

2. Experiment

The measurements have been carried out using the Innsbruck SIFDT apparatus of conventional design (description in [25,28]). The schematic diagram of the "Innsbruck SIFDT" is shown in Fig. 1. In the SIFDT reactant ions were produced in a separated low pressure electron impact ion source. Ions SH^+ and SiH^+ were produced from H_2S and SiH_4, respectively. The ions were mass selected in a quadrupole mass filter and injected into the flow tube via a venturi-type inlet. He at a pressure 0.14–0.4 Torr was used as a buffer gas in the present experiments.

In the first "thermalization" part of the drift tube, a very weak electric field was maintained (E/N is typically <10 Td; 1 Td $= 10^{-17}$ V cm^2) to keep collision energy of the ions with the buffer gas atoms below 0.1 eV. It was assumed that in this region internal excitation of injected ions is quenched. Thermalized reactant ions then enter the downstream region. The reactant gas was introduced to this region and reacted with ions at collision energy corresponding to applied value of E/N. The relative number densities of reactant and product ions were monitored with second, downstream, quadrupole mass spectrometer as a function of the flow rate of the added neutral reactant. The reactant ion/reactant neutral KE_{CM}, was derived by means of the Wannier expression (for details see [29,30]). Mobility of SH^+ and SiH^+ reactant ions in He required for calculations of KE_{CM} was measured in the present experiment. Just for demonstration the obtained reduced mobility of SH^+ vs. E/N is plotted in Fig. 2.

Established methods of data analyses have been used to determine the reaction rate coefficients and product branching ratios. The accuracy of the obtained reaction rate coefficients is ±30% as it is usual for swarm experiments of the SIFDT type.

3. Results and discussion

The reaction rate coefficients and the product branching ratios have been measured for four ion–molecule reactions; reaction of protonated sulfur SH^+ with CH_4 and C_2H_2 and reaction of protonated silicon SiH^+ with C_2H_2 and NH_3. The KE_{CM} was varied from near thermal values (∼0.05 eV) to about 2 eV in our experiment. All four reactions studied

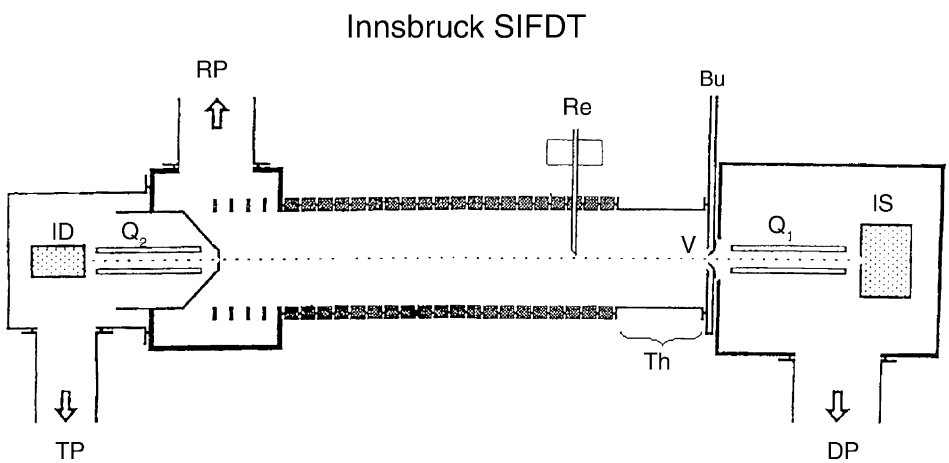

Fig. 1. The Innsbruck selected ion flow drift tube (SIFDT). Q_1, Q_2, quadrupole mass filter; IS, ion source; Th, thermalization region; ID, ion detector; RP, roots pump; TP, turbo pump; DP, diffusion pump; Re, reactant inlet; V, ventury type inlet.

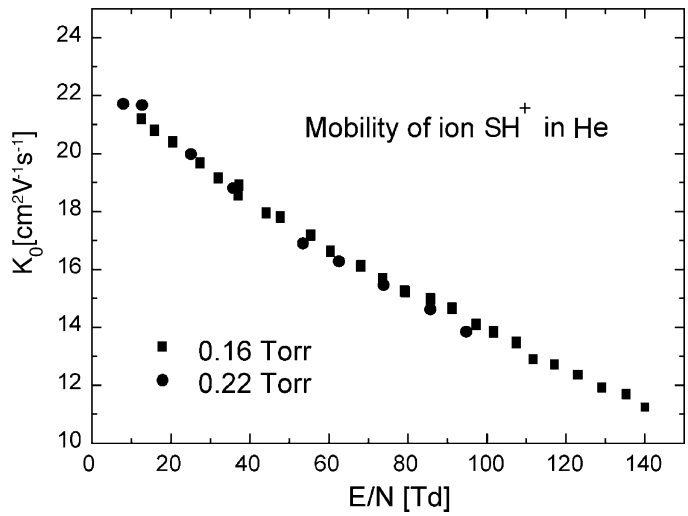

Fig. 2. The reduced mobility of SH^+ ion in He ($1\,Td = 10^{-17}\,V\,cm^2$).

are fast (i.e., they proceed almost at the collisional rate) at near thermal energies and the reaction rate coefficients of all reactions studied decrease with KE_{CM} increasing up to 2 eV. We did not observe a pressure dependence of measured rate coefficients or branching ratios of the product ions.

3.1. The reaction of SH^+ with CH_4

When producing SH^+ from SH_2, we observed in the primary SH^+ signal also a considerable "parasite" signal of $SH_2{}^+$ (not exceeding 15% of the SH^+ signal). Partly this was because of the suppression of the resolution of the injection mass spectrometer in order to obtain a higher SH^+ ion signal with minimal formation of S^+ ions at injection entry port. Fortunately, the $SH_2{}^+$ does not react with CH_4, therefore, it has been possible to determine both the rate coefficient and the product branching ratio. We observed two product ions $SCH_3{}^+$ and $CH_3{}^+$ with a branching ratio dependent on KE_{CM} (Fig. 3). The reaction can be written:

$$\begin{aligned} SH^+ + CH_4 &\rightarrow SCH_3{}^+ + H_2 \\ &\rightarrow CH_3{}^+ + SH_2 \end{aligned} \qquad (5)$$

The measured reaction rate coefficient, k, for different pressures is plotted vs. KE_{CM} in Fig. 4. Note the good agreement with the thermal data obtained in previous experiments ($k = 3.8 \times 10^{-10}$ and $k = 5.4 \times 10^{-10}\,cm^3\,s^{-1}$ in [17,31], respectively). The coefficient k_L indicates the value of a collisional rate coefficient as calculated from simple Langevin theory. Note in Fig. 3 that at low energies the $SCH_3{}^+$ is the dominant product (this is in agreement with thermal data of Smith et al. [31]). With increasing KE_{CM} the product branching ratio changes and at energies over 1 eV the $CH_3{}^+$ is dominant. From the product branching

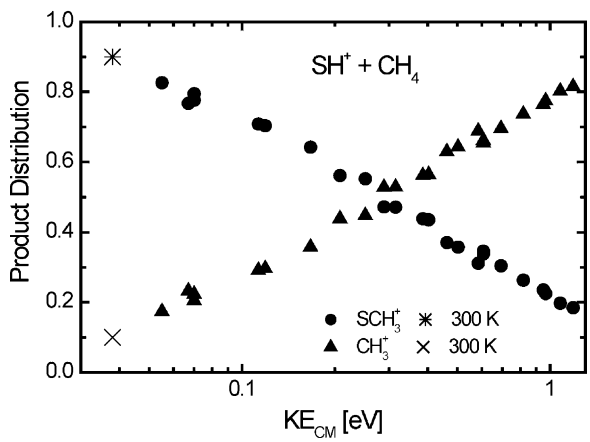

Fig. 3. Product branching ratio of the reaction of SH^+ with CH_4. Stars indicate previous thermal data obtained by Smith et al. [31].

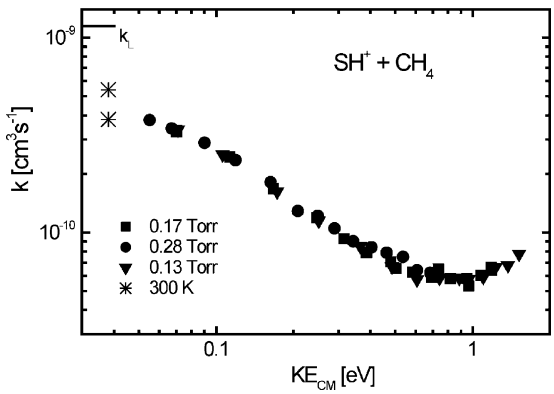

Fig. 4. The reaction rate coefficient of the reaction of SH^+ with CH_4. Different buffer gas pressures are indicated by different symbols. The coefficient k_L indicates the collisional rate coefficient calculated according simple Langevin theory. Stars indicate thermal data obtained in thermal experiments [17,31].

ratio the partial reaction rate coefficients for both channels have been determined and are plotted in Fig. 5 together with the total rate coefficient (total rate coefficient is plotted by solid symbols). From Fig. 5, it can be seen that only the production of SCH_3^+ (exothermic by 3 kcal mol^{-1}) has negative energy dependence. The dotted line represents the fit of the data for the channel producing SCH_3^+ by the function (3) yielding parameters $m = 1.35$, $KE_{CM1} = 0.04$ eV, and

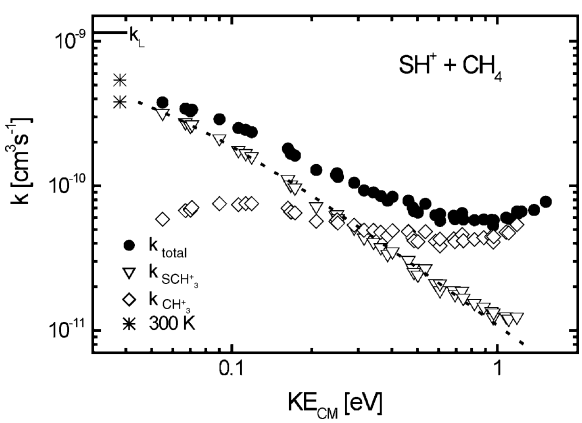

Fig. 5. The partial reaction rate coefficients corresponding to production of SCH_3^+ and CH_3^+ ions. Stars indicate thermal data obtained in SIFT experiments [17,31]. Dotted line indicates fit by formula (3). The closed circles are used to plot the total reaction rate coefficient.

$k_1 = 7.9 \times 10^{-10}$ cm^3 s^{-1}. The production of ground state CH_3^+ ions is expected to be thermoneutral, so that the reaction rate coefficient is nearly constant over the covered energy range.

3.2. The reaction of SH^+ with C_2H_2

The reactant ions were produced by electron impact from SH_2. In order to increase the signal of the primary ions to a reasonable level, the resolution of the source mass spectrometer was suppressed. Because of that the primary ion signal contained traces of S^+ (not exceeding 5% of the SH^+ signal) and SH_2^+ (not exceeding 15% of the SH^+ signal). However, SH_2^+ ions react only slowly with C_2H_2 and the reaction rate coefficient and product branching ratio of the reaction of S^+ with C_2H_2 is known [14]. This allows writing the title reaction as:

$$\begin{aligned} SH^+ + C_2H_2 &\rightarrow SC_2H_2^+ + H \\ &\rightarrow C_2H_3^+ + S \end{aligned} \quad (6)$$

The total reaction rate coefficient k of the reaction (6) vs. KE_{CM} as measured in the present experiment is plotted in Fig. 6 (solid symbols); different pressures of

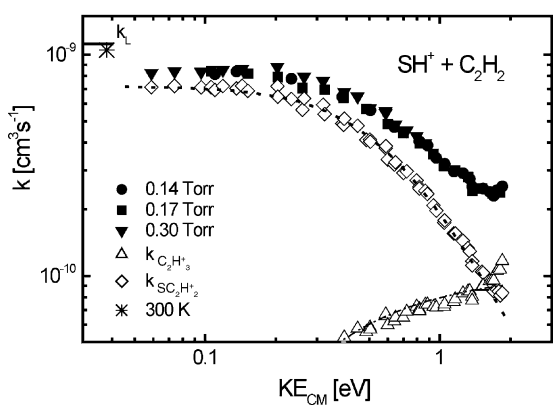

Fig. 6. The total and partial reaction rate coefficients, corresponding to production of ions $SC_2H_2^+$ and $C_2H_3^+$ in the reaction of SH^+ with C_2H_2. The dotted line indicates a fit by formula (3). Different buffer gas pressures are indicated by different symbols. k_L is collisional rate coefficient calculated according simple Langevin theory. Star indicates thermal data taken from compilation of Anicich [17]. The dash-dotted line indicates a fit by Arrhenius function.

the buffer gas (He) are indicated by different symbols. Note that difference between the thermal value and limiting value of our data at near thermal energy is less than 25%, i.e., in range of expected experimental error. The symbols (◇) and (△) in Fig. 6 indicate the partial reaction rate coefficients calculated from the measured branching ratio and the overall rate coefficient. It can be found (using e.g. [32]) that production of $SC_2H_2^+$ is exothermic ($\Delta H = -55.4\,\mathrm{kcal\,mol^{-1}}$) and production of $C_2H_3^+$ is slightly endothermic ($\Delta H = 8.7\,\mathrm{kcal\,mol^{-1}}$).

We assume that the production of $SC_2H_2^+$ ions proceeds via formation of an intermediate complex (and the energy dependence of its reaction rate coefficient is given by formulas (2) and (3)). We also assume that the endothermic production of $C_2H_3^+$ has an Arrhenius type energy dependence of reaction rate coefficient given by the formula:

$$k = k_a \exp\left(-\frac{3E_a}{2\mathrm{KE_{CM}}}\right) \quad (7)$$

where k_a is a constant and E_a is the Arrhenius activation energy [25,33]. The factor 3/2 is from the relation between $\mathrm{KE_{CM}}$ and temperature (for details of this relation in drift tube experiments see discussion in [30,34,35]). The data for the partial rate coefficient of the endothermic channel (triangles) has been fitted by the function (7) is indicated by the dash-dotted line in Fig. 6. The fit yields values $k_a = 5.6 \times 10^{-11}\,\mathrm{cm^3\,s^{-1}}$ and $E_a = 0.19\,\mathrm{eV}$. The dotted line in Fig. 6 represents the fit of the partial reaction rate coefficient of the exothermic channel by formula (3). The parameters obtained from the fit are: $m = 2.0$, $\mathrm{KE_{CM1}} = 0.6\,\mathrm{eV}$, and $k_1 = 7.2 \times 10^{-10}\,\mathrm{cm^3\,s^{-1}}$. In order to manifest superior quality of the fit, we show in Fig. 7 the log-log plot of $((k_1/k) - 1)$ vs. $\mathrm{KE_{CM}}$ (Section 1). The solid line represents the fit yielding the same values of m and $\mathrm{KE_{CM1}}$ as obtained from the fit of k by using formula (3).

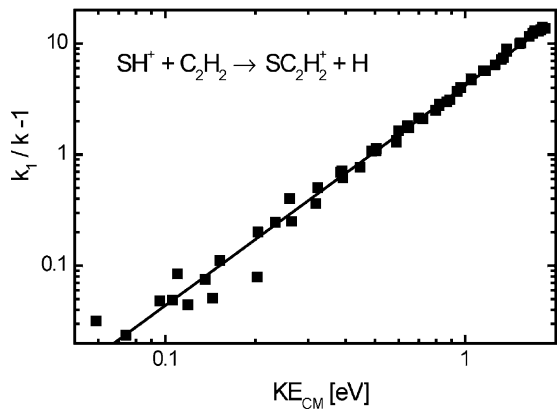

Fig. 7. Plot of $((k_1/k) - 1)$ vs. $\mathrm{KE_{CM}}$. The partial reaction rate coefficient, k, corresponds to the production of $SC_2H_2^+$ in the reaction of SH^+ with C_2H_2. The constant k_1 is obtained by the fit of the corresponding data plotted in Fig. 6.

3.3. The reaction of SiH^+ with C_2H_2

The primary ions were produced from SiH_4 in the low pressure ion source. In the mass spectrum of injected "primary" ions, we observed beside the primary ion signal (SiH^+) also the ions Si^+, SiH_2^+ and SiH_3^+ were present (not exceeding 3–5% of the SiH^+ signal). The presence of already mentioned "parasite ions" leads to more complicated product analysis. However, using the knowledge of the product branching ratios and rate coefficients of reactions of these "parasite ions" it was possible to conclude that the dominant product of the reaction of SiH^+ with C_2H_2 is the SiC_2H^+ ion (we cannot exclude very small channels producing $SiC_2H_2^+$ and $SiC_2H_3^+$). Hence, the reaction scheme can be written as:

$$SiH^+ + C_2H_2 \rightarrow SiC_2H^+ + H_2 \quad (8)$$

In Fig. 8, the measured reaction rate coefficient k of reaction (8) is plotted vs. $\mathrm{KE_{CM}}$. Note the disagreement of our data with thermal value obtained by Lampe et al. using his tandem mass spectrometer (the value indicated by star was taken from [17]). Also the product branching ratio reported by Lampe differs significantly from the product branching ratio obtained in the present experiment. Lampe reports [17] only 47% of the product SiC_2H^+ and in addition to our observation he reports 53% of $SiC_2H_2^+$. The dotted line in Fig. 8 indicates the fit of the data by the formula (3). The parameters obtained

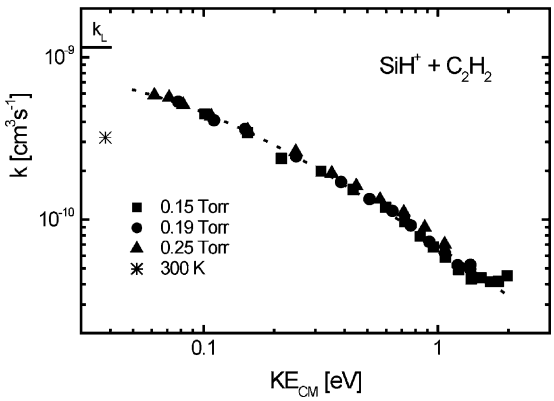

Fig. 8. The reaction rate coefficient of the reaction of SiH^+ with C_2H_2. Different buffer gas pressures are indicated by different symbols. k_L is the rate coefficient calculated according simple Langevin theory. The dotted line indicates a fit by formula (3). The star indicates previous data obtained at 300 K [17].

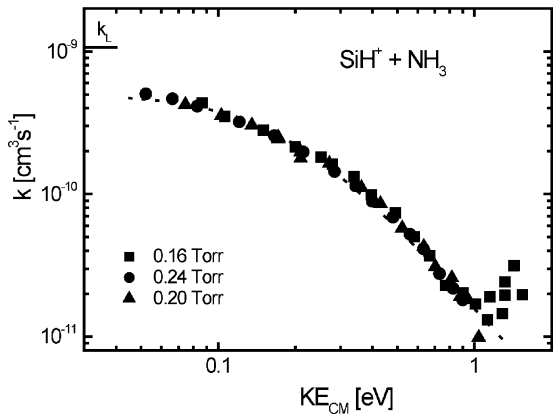

Fig. 9. The reaction rate coefficient of the reaction of SiH^+ with NH_3. The dotted line indicates a fit by formula (3).

by the fit are: $m = 1.07$, $KE_{CM1} = 0.09\,eV$, $k_1 = 9.6 \times 10^{-10}\,cm^3\,s^{-1}$.

3.4. The reaction of SiH^+ with NH_3

Similar to the case of the reaction of SiH^+ with C_2H_2 it has been very difficult to produce a pure signal of the SiH^+ ion. NH_4^+ and $SiNH_2^+$ were observed as product ions. Due to the presence of the "parasite primary ions" (Si^+, SiH_2^+ and SiH_3^+, not exceeding 3–5% of the SiH^+ signal) it was not simple to determine the product branching ratio. However, because it is known from our previous study [2] that the reaction of the ground state Si^+ ion with NH_3 yields only product $SiNH_2^+$ in the whole energy range covered in the present study, we were able to estimate that the maximal abundance of the $SiNH_2^+$ product ion does not exceeding 15%. The reaction of SiH^+ with ammonia then can be written:

$$\begin{aligned} SiH^+ + NH_3 &\rightarrow SiNH_2^+ + H_2 \\ &\rightarrow NH_4^+ + Si \end{aligned} \qquad (9)$$

The measured reaction rate coefficient, k, is plotted vs. KE_{CM} in Fig. 9. The fit yields parameters: $m = 2.0$, $KE_{CM1} = 0.18\,eV$, $k_1 = 5.0 \times 10^{-10}\,cm^3\,s^{-1}$. The reaction rate coefficient increases with increasing KE_{CM} above 1 eV. Despite a careful analysis of the mass spectrometer data, we did not observe changes of the product ions correlated to this increase of the rate coefficient.

4. Concluding remarks

We have investigated the energy dependencies of the reaction rate coefficients and the product branching ratios of the reactions of SH^+ with CH_4 and C_2H_2 and the reactions of SiH^+ with C_2H_2 and NH_3. All reactions studied have very strong negative energy dependencies of the reaction rate coefficients. Quality of the fits of energy dependencies of the reaction rate coefficients by function (3) supports our assumption that these reactions pass through formation of intermediate complexes.

Using Innsbruck SIFDT, we recently measured over 20 reactions [2,13–15,22,23,30] of Si^+, SiH^+, S^+ and SH^+ ions with small molecules containing C, N, and O. In a majority of these reactions, new bonds between Si and S on one side and C, N, O on another side were formed. We observed in these reactions negative energy dependence of reaction rate coefficient on KE_{CM}. The studied reactions are binary, independent on He pressure the reaction [15] of $Si^+(^2P)$ with C_2H_4 being the only exception. In this reaction, we observed the

binary channel (products $SiC_2H_3^+$/H) and two ternary channels: collisional stabilization (product $SiC_2H_4^+$) and collisional dissociation (products $SiC_2H_3^+$/H).

Acknowledgements

J.G., P.Z. and A.L. wish to express their thankfulness for the hospitality during visits at the Institute für Ionenphysik in Innsbruck. In particular, we are very thankful to our dear friend Werner Lindinger for hospitality, encouraging discussions and support of our work. Thanks for financial support are due to GACR (202/99/D061, 205/02/0610, 202/02/0948), GAUK (146/2000 and 171/2000 B FYZ MFF). The construction of the ion source was supported in part by the VW foundation (Schwerpunkt intra- and inter-moleculare Electronenubertragung, Az.: I/72 593).

References

[1] A.E. Ketvirtis, D.K. Bohme, A.C. Hopkinson, J. Phys. Chem. 99 (1995) 16121.
[2] J. Glosík, P. Zakouřil, W. Lindinger, J. Chem. Phys. 103 (1995) 6490.
[3] B.K. Decker, L.M. Babcock, N.G. Adams, J. Phys. Chem. 104 (2000) 801.
[4] A.E. Ketvirtis, D.K. Bohme, A.C. Hopkinson, J. Phys. Chem. 103 (1999) 11161.
[5] C. Barrientos, A. Largo, J. Phys. Chem. 96 (1992) 5808.
[6] S.W. Chiu, W.K. Li, W. Tzeng, C.Y. Ng, J. Chem. Phys. 97 (1992) 6557.
[7] B.K. Decker, N.G. Adams, L.M. Babcock, Int. J. Mass Spectrom. 187 (1999) 727.
[8] D. Smith, N.G. Adams, K. Giles, E. Herbst, Astron. Astrophys. 200 (1988) 191.
[9] T.J. Millar, in: D.K. Bohme, E. Herbst, N. Kaifu, S. Saito (Eds.), Chemistry and Spectroscopy of Interstellar Molecules, University of Tokyo Press, 1990.
[10] D. Smith, Chem. Rev. 92 (1992) 1473.
[11] E. Herbst, T.J. Miller, S. Wlodek, D.K. Bohme, Astron. Astrophys. 222 (1989) 205.
[12] H.A. Wootten, NRAO, http://WWW.cv.nrao.edu/~awootten/allmols.html, 2002.
[13] J. Glosík, P. Zakouřil, W. Lindinger, Int. J. Mass Spectrom. Ion Process. 149/150 (1995) 499.
[14] P. Zakouřil, J. Glosík, V. Skalský, W. Lindinger, J. Phys. Chem. 99 (1995) 15890.
[15] J. Glosík, P. Zakouřil, W. Lindinger, Int. J. Mass Spectrom. Ion Process. 145 (1995) 155.
[16] D.K. Bohme, Adv. Gas Phase Ion Chem. 1 (1992) 225.
[17] V.G. Anicich, J. Phys. Chem. Ref. Data 22 (1993) 1469.
[18] R.C. Dunbar, in: C.Y. Ng, T. Baer, I. Powis (Eds.), Unimolecular and Bimolecular Ion–Molecule Reaction Dynamics, Wiley, New York, 1994.
[19] J. Troe, in: M. Baer, C.Y. Ng (Eds.), State Selected and State to State Ion–Molecule Reaction Dynamics, Wiley, New York, 1992.
[20] C.E. Klots, in: C.Y. Ng, T. Baer, I. Powis (Eds.), Unimolecular and Bimolecular Ion–Molecule Reaction Dynamics, Wiley, New York, 1994.
[21] W. Forst, Theory of Unimolecular Reactions, Academic Press, New York, 1973.
[22] J. Glosík, P. Zakouřil, W. Lindinger, Czech. J. Phys. 48 (1998) 29.
[23] G. Bano, A. Luca, J. Glosík, P. Zakouřil, W. Lindinger, Czech. J. Phys. 50/S3 (2000) 251.
[24] E.E. Ferguson, J. Chem. Phys. 90 (1986) 731.
[25] J. Glosík, W. Freysinger, A. Hansel, P. Spanel, W. Lindinger, J. Chem. Phys. 98 (1993) 6995.
[26] J. Glosík, V. Skalsky, C. Praxmarer, D. Smith, W. Freysinger, W. Lindinger, J. Chem. Phys. 101 (1994) 3792.
[27] W.J. Chesnavich, M.T. Bowers, in: M.T. Bowers (Ed.), Gas Phase Ion Chemistry, Vol. 1, Academic Press, New York, 1979.
[28] W. Federer, H. Ramler, H. Villinger, W. Lindinger, Phys. Rev. Lett. 54 (1985) 540.
[29] G.H. Wannier, Bell Syst. Tech. J. 32 (1953) 170.
[30] J. Glosík, V. Skalsky, W. Lindinger, Int. J. Mass Spectrom. Ion Process. 134 (1994) 67.
[31] D. Smith, N.G. Adams, W. Lindinger, J. Chem. Phys. 75 (1981) 3365.
[32] D.R. Lide (Ed.), CRC Handbook of Chemistry and Physics, 71st Edition, CRC Press, Boca Raton, 1991.
[33] P.W. Atkins, Physical Chemistry, 3rd Edition, Oxford University Press, Oxford, 1988.
[34] L.A. Viehland, S.L. Lin, E.A. Mason, Chem. Phys. 54 (1981) 341.
[35] L.A. Viehland, E.A. Mason, Chem. Phys. 99 (1993) 1457.